

Parameters that control lithospheric-scale thermal localization on terrestrial planets

Fabio Crameri¹ and Boris J. P. Kaus¹

Received 16 February 2010; revised 31 March 2010; accepted 12 April 2010; published 14 May 2010.

[1] Shear-heating induced localization has been suggested as a potentially important mechanism for breaking the lithosphere. Yet, the physical parameters that control the onset of this instability remain unclear. We therefore performed systematic 2-D simulations of visco-elasto-plastic lithospheric deformation in which we addressed the effects of various parameters and we found that a sharp transition exists between localizing and non-localizing regimes. In a next step we develop a semi-analytical model that combines scaling laws with a 1-D lithospheric deformation model. We show that the 1-D model successfully predicts the occurrence of shear localization in 2-D models, if the thickness of the plastically deforming part of the (lower) lithosphere is employed as characteristic length-scale. An application of the 1-D model to the terrestrial planets shows that this type of shear-localization is expected to occur most readily on Earth. **Citation:** Crameri, F., and B. J. P. Kaus (2010), Parameters that control lithospheric-scale thermal localization on terrestrial planets, *Geophys. Res. Lett.*, 37, L09308, doi:10.1029/2010GL042921.

1. Introduction

[2] The physical mechanisms that are responsible for the occurrence of plate tectonics on Earth is one of the most important unresolved topics in geodynamics [Bercovici, 2003]. Although considerable progress has been made over the last decade, numerical models in which plate-like behavior emerges from a single convecting system remain scarce and require in all cases some form of a yield stress to break the stagnant lid, which would form otherwise [e.g., van Heck and Tackley, 2008]. The process of rupturing the stagnant lid seems to be one of the key processes in these models, and the parameterized manner in which yielding is typically implemented requires the use of yield stress values that are smaller than expected on the basis of laboratory experiments [Kohlstedt et al., 1995]. A number of researchers have therefore concentrated on processes that might result in lithospheric-scale shear zones. The main goal is to find a process that results in localized deformation in the mantle lithosphere, where the maximum strength of rocks is given by Peierls or low-temperature plasticity rather than by a (self-localizing) Byerlee yield stress as in the upper crust [Kaus and Podladchikov, 2006]. Additional weakening mechanisms are thus required [Montési and Zuber, 2002]

and might be given by grain size reduction under rapid cooling [Braun et al., 1999], grain boundary sliding [Precigout and Gueydan, 2009], two-phase flow and void generation [Landuyt and Bercovici, 2009], lattice preferred orientation of olivine [Tommasi et al., 2009], weak layer interconnection [Montési, 2007] or shear heating.

[3] Here, we focus on shear heating as it is one of the simplest weakening mechanisms. Over the last two decades this process has been studied with one [Braeck and Podladchikov, 2007; Kameyama et al., 1999; Ogawa, 1987] and two-dimensional models [Burg and Schmalholz, 2008; Kaus and Podladchikov, 2006; Regenauer-Lieb et al., 2001; Schmalholz et al., 2009]. The mechanism was suggested to be responsible for deep intra-slab earthquakes [Kameyama et al., 1999; Ogawa, 1987] for the ultimate strength of materials [Braeck and Podladchikov, 2007], and can explain the occurrence of shear-zones alongside pseudo-tachylites [John et al., 2009]. Whereas two-dimensional models illustrated that this mechanism might indeed cause lithospheric-scale shear-zones, the large number of model parameters makes it difficult to estimate which of the model parameters are of key importance for the localization process [Regenauer-Lieb et al., 2001; Schmalholz et al., 2009]. Therefore, Kaus and Podladchikov [2006] performed extensive numerical simulations and used those to derive scaling laws for the onset of localization. Yet, the viscous rheology of rocks in their study was approximated with a (linear) Frank-Kamenetskii rheology and the rheological stratification of the lithosphere was not taken into account. The purpose of this study is to develop a method that predicts the onset of localization for a visco-elasto-plastic lithosphere with arbitrary rheological stratification and realistic creep rheologies.

2. Methodology and Model Setup

2.1. Mathematical Formulation

[4] The Boussinesq equations for a slowly deforming Maxwell visco-elasto-plastic lithosphere are given by

$$\begin{aligned} \dot{\epsilon}_{ii} &= 0 \\ -\frac{\partial P}{\partial x_i} + \frac{\partial \tau_{ij}}{\partial x_j} &= \rho_0(1 - \alpha(T - T_0))g_i \\ \dot{\epsilon}_{ij} &= \frac{\tau_{ij}}{2\eta} + \frac{1}{2G} \frac{D\tau_{ij}}{Dt} + \lambda \frac{\partial Q}{\partial \sigma_{ij}} \\ \frac{D\tau_{ij}}{Dt} &= \frac{\partial \tau_{ij}}{\partial t} + v_k \frac{\partial \tau_{ij}}{\partial x_k} - W_{ik} \tau_{kj} + \tau_{ik} W_{kj} \\ \rho c_p \left(\frac{\partial T}{\partial t} + v_k \frac{\partial T}{\partial x_k} \right) &= \frac{\partial}{\partial x_i} \left(k \frac{\partial T}{\partial x_i} \right) + H + \tau_{ij} \left(\dot{\epsilon}_{ij} - \frac{1}{2G} \frac{D\tau_{ij}}{Dt} \right) \end{aligned} \quad (1)$$

¹Geophysical Fluid Dynamics, Institute of Geophysics, ETH Zurich, Zurich, Switzerland.

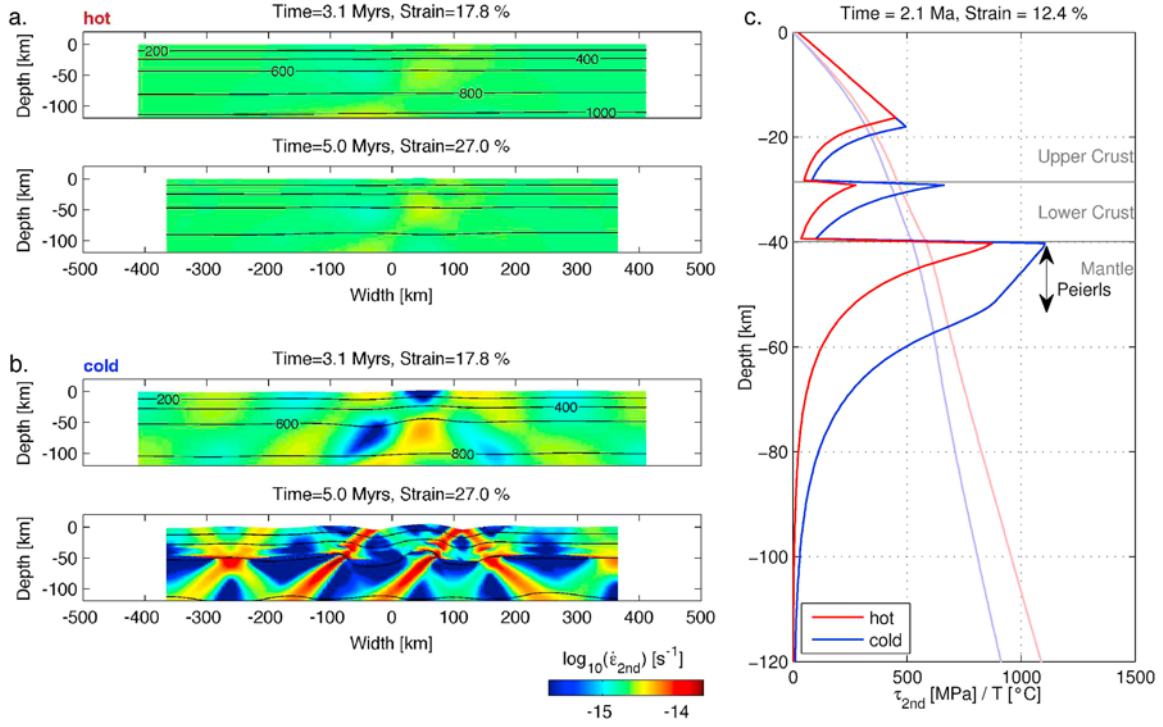


Figure 1. Temporal evolution of second invariant of strain rate plotted for (a) hot lithosphere ($T_{bot} = 1200^\circ\text{C}$) and (b) cold lithosphere ($T_{bot} = 1000^\circ\text{C}$), deformed with $\dot{\epsilon}_{bg} = 2 \cdot 10^{-15}$. (c) Maximum differential stress and temperature computed for a homogeneous “hot” and “cold” lithosphere.

where $\dot{\epsilon}_{ij} = \frac{1}{2} \left(\frac{\partial v_i}{\partial x_j} + \frac{\partial v_j}{\partial x_i} \right)$ is strain-rate, v_i velocity, ρ density, g_i gravitational acceleration, $P = -\sigma_{ii}/3$ pressure, σ_{ij} stress, x_i spatial coordinates, τ_{ij} deviatoric stress, G elastic shear module, $W_{ij} = \frac{1}{2} \left(\frac{\partial v_i}{\partial x_j} - \frac{\partial v_j}{\partial x_i} \right)$ vorticity, t time, $\dot{\lambda}$ the plastic multiplier, Q the plastic flow potential, T temperature, α thermal expansivity, c_p heat capacity, k thermal conductivity, H radioactive heat production and η the effective viscosity. Creep rheology for upper crustal rocks is given by

$$\eta_{eff} = A^{-1/n} (\dot{\epsilon}_{2nd})^{1/n-1} \exp\left(\frac{E}{nRT}\right) \quad (2)$$

where A is a pre-exponential parameter, n the power-law exponent, R the universal gas constant, E the activation energy and $\dot{\epsilon}_{2nd} = (0.5\dot{\epsilon}_{ij}\dot{\epsilon}_{ij})^{0.5}$ the second invariant of the strain rate tensor. The Byerlee brittle strength of upper crustal rocks is approximated by Mohr-Coulomb plasticity, which (in 2-D) is

$$\begin{aligned} F &= \tau^* - \sigma^* \sin(\phi) - c \cos(\phi) \\ Q &= \tau^* \\ \dot{\lambda} &\geq 0, F \leq 0, \dot{\lambda}F = 0 \end{aligned} \quad (3)$$

where $\tau^* = ((0.5(\sigma_{xx} - \sigma_{zz}))^2 + \sigma_{xz}^2)^{0.5}$, $\sigma^* = -0.5(\sigma_{xx} - \sigma_{zz})$, c cohesion and ϕ the internal angle of friction (taken to be 30° here). Under larger confining pressures, Byerlee's law breaks down and the yield strength is described by “Peierls” or “low-temperature” plasticity. Here we adopt the formulation of

Goetze and Evans [1979], which is applied for differential stresses that are larger than 200 MPa:

$$\tau_{ij} = \frac{\sigma_0}{\dot{\epsilon}_{2nd} \sqrt{3} \left(1 - \sqrt{RT/H_0 \ln(\sqrt{3}\dot{\epsilon}_0/2\dot{\epsilon}_{2nd})} \right)} \dot{\epsilon}_{ij} \quad (4)$$

with $\dot{\epsilon}_0 = 5.7 \cdot 10^{11} \text{ s}^{-1}$, $\sigma_0 = 8.5 \cdot 10^9 \text{ Pa}$, $H_0 = 525 \text{ kJ/mol}$.

2.2. Numerical Methodology and Model Setup

[5] The 2-D governing equations are solved with the Lagrangian particle-in-cell finite element code MILAMIN_VEP, which includes re-meshing and uses an iterative penalty method to enforce incompressibility [e.g., see Kaus *et al.*, 2009]. The code has been benchmarked with various analytical solutions and versus the results of FEMS-2D for selected simulations by Schmalholz *et al.* [2009]. In addition, we developed a 1-D code that computes stress and temperature evolution in a lithosphere subjected to pure-shear compression (in the presence of shear heating). The energy equation is solved with a finite difference method, and results are in good agreement with the 2-D code (for laterally homogeneous setups).

[6] Our setup considers a $1000 \times 120 \text{ km}$ lithosphere with a free surface and kinematic side and lower boundaries that is subjected to homogeneous compression with prescribed strain rate $\dot{\epsilon}_{bg}$. The lithosphere consists of an upper/lower crust and mantle lithosphere, and has an initial steady-state temperature with zero-flux side boundary conditions and isothermal upper and lower boundaries. In order to localize deformation, the bottom temperature T_{bot} is slightly (30 K) larger at the right side of the model. Larger perturbations

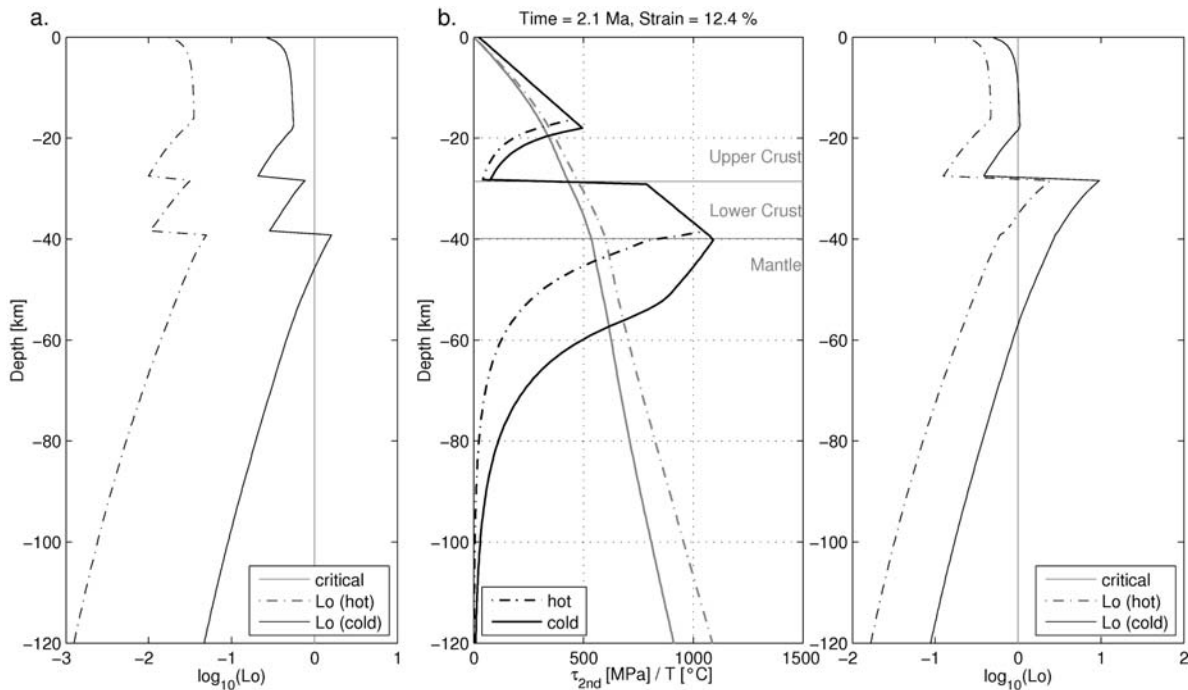


Figure 2. (a) Localization number for the simulations of Figure 1. (b) Maximum differential stress and temperature for simulations with a strong lower crust (left), and localization number versus depth (right) both for “hot” and “cold” geotherms.

decrease the strain at which localization initiates, but not its overall pattern. Quadrilateral Q_2P_{-1} elements with a resolution of 401×161 nodes are employed in all cases. A test with 1204×484 nodes yielded nearly identical results with respect to the onset time and overall patterns of lithospheric-scale shear localization, although brittle localization in the upper crust was more pronounced. Material parameters are the same as those employed by *Burg and Schmalholz* [2008], and consist in most cases of a dry quartzitic upper crust, a diabase lower crust and a wet olivine mantle (see Table 1 in Text S1).¹

3. Results

3.1. 2-D Numerical Simulations

[7] We have performed over 200 2-D numerical simulations in which we systematically varied T_{bot} , $\dot{\epsilon}_{bg}$, the thickness of lithospheric layers as well as the rheology. As *Schmalholz et al.* [2009] we find that deformation can occur by pure-shear thickening, lithospheric-scale folding or lithospheric-scale shear localization. Snapshots from typical simulations are shown on Figure 1. The “hot” model results in pure-shear thickening of the lithosphere with little internal deformation (Figure 1a). The “cold” model, on the other hand, initially deforms homogeneously but develops localized shear zones in the mantle lithosphere after 15% of total strain (Figure 1b). With ongoing strain, shear-zones narrow and take up most subsequent deformation.

[8] In order to understand the differences between these two simulations it is instructive to compute the evolution of

stress and temperature in a 1-D homogeneous lithosphere. Whereas maximum stresses in the upper crust are similar in both simulations, the “cold” case has larger stresses in the mantle lithosphere, such that the dominant deformation mechanism here is Peierls creep (Figure 1c).

3.2. Semi-Analytical Localization Model

[9] *Kaus and Podladchikov* [2006] showed that the onset of localization for kinematic boundary conditions is given by $\dot{\epsilon}_{bg} \geq \frac{1.4}{L} \sqrt{\frac{\kappa/\rho c_p}{\eta_0 \gamma}}$, where κ is the thermal diffusion, η_0 the viscosity at temperature T_0 , L a heterogeneity length scale, and γ the temperature-dependence of viscosity in the Frank-Kamenetskii approximation ($\eta = \eta_0 \exp[-\gamma(T - T_0)]$) which can be computed from a power-law creep rheology by $\gamma = E/(nRT_0^2)$ [e.g., *Solomatov and Moresi*, 1996]. Localization thus requires the system to have a heterogeneity length scale that is larger than a critical value $L_c = \frac{1.4}{\dot{\epsilon}_{bg}} \sqrt{\frac{k}{\eta_0 \gamma}}$, where k is the thermal conductivity. One can use this to define as localization condition

$$Lo = \frac{\dot{\epsilon}_{bg} L}{1.4} \sqrt{\frac{\eta_0 \gamma}{k}} = \frac{\dot{\epsilon}_{bg} L}{1.4} \sqrt{\frac{\eta_0 E}{nRT_0^2 k}} \quad (5)$$

which predicts localization for $Lo > 1$. For a given simulation, all parameters in equation (5) are known, with exception of the length scale L . In the 2-D simulations of *Kaus and Podladchikov* [2006], an initial circular inclusion of radius L was emplaced in a homogeneous lithosphere. Yet, in our 2-D simulations such heterogeneity is not present. By analyzing our 2-D simulations, we found a good agreement if the thickness of the Peierls layer is used

¹Auxiliary materials are available in the HTML. doi:10.1029/2010GL042921.

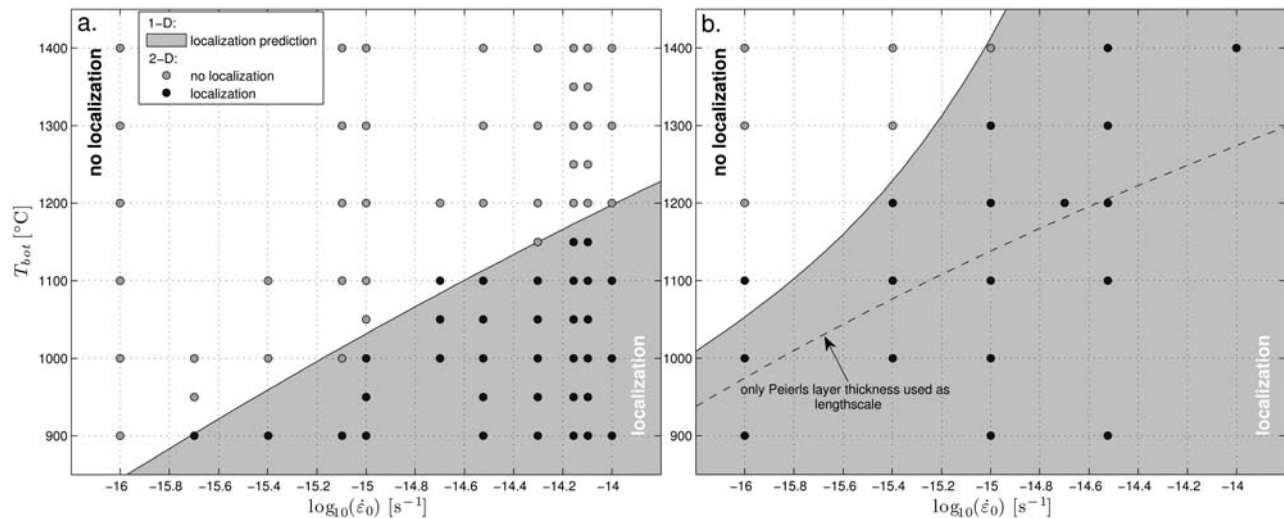


Figure 3. One-dimensional predicted onset of shear localization (black curve, $Lo = 1$) versus finite strain 2-D simulations that resulted in either localization (dark dots) or no localization (light dots). Either (a) a weak or (b) a strong lower crust rheology was employed.

as length scale L in the case of Figure 1. If the lower crust is brittle, L is given by the sum of the Coulomb and Peierls layers. Physically, this implies that the lithosphere develops a system-wide length scale that is significantly larger than the length scale typically employed in localization studies [e.g., *Montési and Zuber, 2002*]. In our case this is probably caused by small amplitude buckling of the strong mantle lithosphere, which induces heterogeneities in the stress field with a length scale on the order of the layer thickness.

[10] With the help of the 1-D deformation code, we can compute Lo (using $\eta_0 = \tau_{2nd}/(2\dot{\epsilon}_{bg})$ in the upper crust and $\eta_0 = \eta_{eff}$ otherwise) as well as L , which are both time-dependent due to visco-elastic stress build-up. A comparison of the maximum Lo in a simulation for the “hot” and “cold” case of Figure 1 reveals that $Lo > 1$ in the mantle lithosphere of the “cold case”, but that $Lo < 1$ for the “hot case” (Figure 2a). If a “strong” lower crustal rheology is used instead, stresses reach brittle yielding in the lower crust. The appropriate length scale here is the thickness of the Peierls layer and the thickness of the brittle lower crust, which predicts localization for both the hot and cold cases (Figure 2b), in agreement with 2-D numerical simulations.

3.3. Localization Predictions Versus 2-D Results

[11] A computation of the critical Lo versus bottom temperature and background strain-rates illustrates that localization is favored in lithospheres that are either relatively cold or rapidly deformed (Figure 3). In a next step, we compared the 1-D predictions with 2-D numerical simulations. For this, we have to define a criterion to distinguish localizing from non-localizing simulations. Several possibilities exist beyond a visual inspection of the strain-rate and viscosity fields. Here, we employ the fact that localization causes offsets of the Moho and use the first derivative of the Moho topography as criteria (with $dz/dx > 4$ indicating localization). A comparison of 1-D predictions and 2-D results show that they are in excellent agreement (Figure 3). If only the thickness of the Peierls layer is used instead of

the thickness of the total (pseudo)-plastic layer, the agreement is less satisfactory (Figure 3b).

4. Application

[12] Next we use our semi-analytical approach to estimate the potential for localization on Earth, Mars and Venus. For simplicity, we use a two-layer setup with a granitic crust and a wet olivine mantle for Earth and a diabase crust and a dry olivine mantle for Mars and Venus, with a half-space initial temperature profile of given cooling age (ignoring radioactive heat production).

[13] The Earth has an average crustal thickness of 30 km and a mantle temperature of 1350 °C with a surface temperature of 0 (or 40) °C. Mars, on the other hand, has a larger crustal thickness of 50 km, a mantle of 1350 °C and a surface temperature of -53 °C [*Breuer and Spohn, 2003*]. Venus has a 30 km thick crust, a mantle temperature of 1350 °C and a significantly larger surface temperature of 466 °C [*Nimmo and McKenzie, 1996*].

[14] Apart from extremely large strain rates at which localization on all planets is equally likely, results show that Earth has the largest potential for shear localization (Figure 4), whereas localization on Mars and Venus is more difficult since the mantle lithospheres have smaller differential stresses. For Mars, this effect is caused by a larger average crustal thickness whereas on Venus the lithosphere is significantly hotter due to the high surface temperatures. Note however that the lithosphere also needs to be shortened by ~20% for localization to occur, and that larger initial perturbations (such as strong steps in lithospheric thickness) facilitate the occurrence of shear localization. More work is thus required to understand whether this mechanism might be responsible for a transition from stagnant-lid to a plate-like mode of convection.

5. Conclusion

[15] We have studied the onset of shear-heating induced shear localization with 2-D numerical models of lithospheric

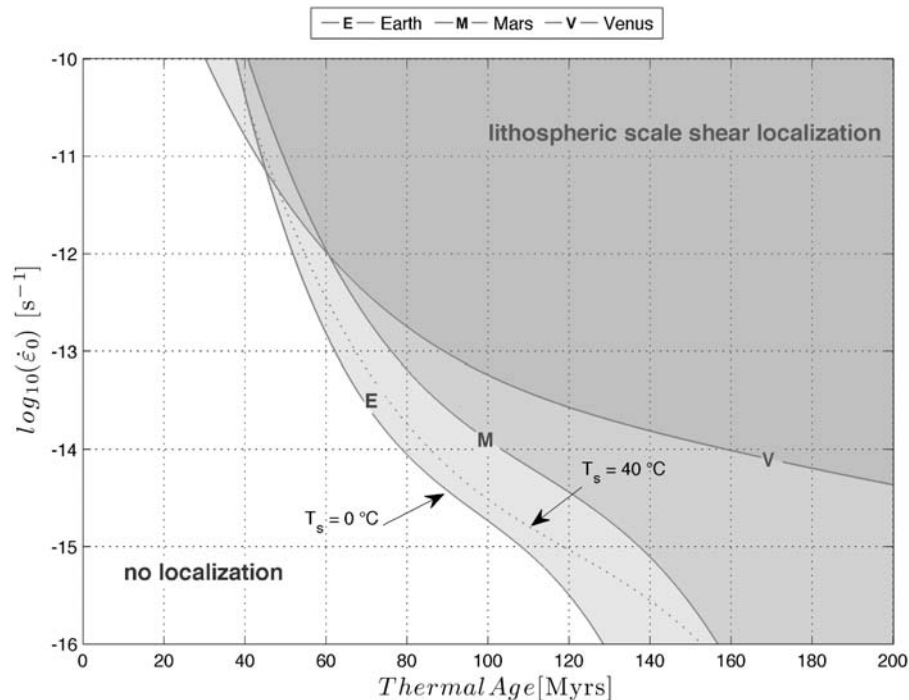


Figure 4. Predicted onset of lithospheric-scale shear localization on Earth (E), Mars (M) and Venus (V), assuming a two-layer lithosphere. Shear localization (grey areas) typically occurs most readily on Earth.

deformation. The models indicate that this mechanism is indeed capable of generating lithospheric-scale shear-zones, which typically initiate in the mantle lithosphere and preferentially occur in cold and rapidly deforming lithospheres. Shear heating is particularly efficient in the strongest parts of the lithosphere (e.g. the upper mantle), where it can lead to shear localization by locally decreasing the viscosity.

[16] In a second step we developed a semi-analytical 1-D model to predict the occurrence of shear-localization in 2-D numerical models. The semi-analytical model combines a 1-D lithospheric deformation code with previously derived scaling laws for the onset of localization. If the thickness of the plastically deforming (Peierls or Peierls/Coulomb) part of the lithosphere is employed as characteristic length scale, we obtain excellent agreement between predictions and 2-D numerical simulations.

[17] An application of the method to the terrestrial planets shows that conditions for localization are most readily reached on Earth for reasonable parameter values.

[18] **Acknowledgments.** We thank Paul Tackley, Stefan Schmalholz and Yuri Podladchikov for stimulating discussions, and an anonymous reviewer for constructive comments. This project has benefitted from the EU Crystal2Plate Marie-Curie training network.

References

Bercovici, D. (2003), The generation of plate tectonics from mantle convection, *Earth Planet. Sci. Lett.*, *205*, 107–121.
 Braeck, S., and Y. Podladchikov (2007), Spontaneous thermal runaway as an ultimate failure mechanism of materials, *Phys. Rev. Lett.*, *98*, 095504.
 Braun, J., J. Chéry, A. Poliakov, D. Mainprice, A. Vauchez, A. Tomassi, and M. Daiginières (1999), A simple parameterization of strain localization in the ductile regime due to grain size reduction: A case study for olivine, *J. Geophys. Res.*, *104*(B11), 25,167–25,181, doi:10.1029/1999JB900214.

Breuer, D., and T. Spohn (2003), Early plate tectonics versus single-plate tectonics on Mars: Evidence from magnetic field history and crust evolution, *J. Geophys. Res.*, *108*(E7), 5072, doi:10.1029/2002JE001999.
 Burg, J. P., and S. M. Schmalholz (2008), Viscous heating allows thrusting to overcome crustal-scale buckling: Numerical investigation with application to the Himalayan syntaxes, *Earth Planet. Sci. Lett.*, *274*(1–2), 189–203.
 Goetze, C., and B. Evans (1979), Stress and temperature in the bending lithosphere as constrained by experimental rock mechanics, *Geophys. J. R. Astron. Soc.*, *59*, 463–478.
 John, T., et al. (2009), Generation of intermediate-depth earthquakes by self-localizing thermal runaway, *Nat. Geosci.*, *2*(2), 137–140.
 Kameyama, C., et al. (1999), Thermal-mechanical effects of low temperature plasticity (the Peierls mechanism) on the deformation of a viscoelastic shear zone, *Earth Planet. Sci. Lett.*, *168*, 159–162.
 Kaus, B. J. P., and Y. Y. Podladchikov (2006), Initiation of localized shear zones in viscoelastoplastic rocks, *J. Geophys. Res.*, *111*, B04412, doi:10.1029/2005JB003652.
 Kaus, B. J. P., et al. (2009), Lithospheric stress-states predicted from long-term tectonic models: influence of rheology and possible application to Taiwan, *J. Asian Earth Sci.*, *36*(1), 119–134.
 Kohlstedt, D. L., B. Evans, and S. Mackwell (1995), Strength of the lithosphere: Constraints imposed by laboratory measurements, *J. Geophys. Res.*, *100*(B9), 17,587–17,602.
 Landuyt, W., and D. Bercovici (2009), Formation and structure of lithospheric shear zones with damage, *Phys. Earth Planet. Inter.*, *175*(3–4), 115–126.
 Montési, L. G. J. (2007), A constitutive model for layer development in shear zones near the brittle-ductile transition, *Geophys. Res. Lett.*, *34*, L08307, doi:10.1029/2007GL029250.
 Montési, L. G. J., and M. T. Zuber (2002), A unified description of localization for application to large-scale tectonics, *J. Geophys. Res.*, *107*(B3), 2045, doi:10.1029/2001JB000465.
 Nimmo, F., and D. McKenzie (1996), Modelling plume-related uplift, gravity and melting on Venus, *Earth Planet. Sci. Lett.*, *145*(1–4), 109–123.
 Ogawa, M. (1987), Shear instability in a viscoelastic material as the cause of deep focus earthquakes, *J. Geophys. Res.*, *92*(B1), 13,801–13,810.
 Precigout, J., and F. Gueydan (2009), Mantle weakening and strain localization: Implications for the long-term strength of the continental lithosphere, *Geology*, *37*(2), 147–150.
 Regenauer-Lieb, K., et al. (2001), The initiation of subduction: Criticality by addition of water?, *Science*, *294*, 578–580.

- Schmalholz, S. M., et al. (2009), Stress-strength relationship in the lithosphere during continental collision, *Geology*, 37(9), 775–778.
- Solomatov, V. S., and L. N. Moresi (1996), Stagnant lid convection on Venus, *J. Geophys. Res.*, 101(E2), 4737–4753.
- Tommasi, A., et al. (2009), Structural reactivation in plate tectonics controlled by olivine crystals anisotropy, *Nat. Geosci.*, 2, 423–427, doi:410.1038/NCEO1528.
- van Heck, H. J., and P. J. Tackley (2008), Planforms of self-consistently generated plates in 3D spherical geometry, *Geophys. Res. Lett.*, 35, L19312, doi:10.1029/2008GL035190.

F. Cramer and B. J. P. Kaus, Geophysical Fluid Dynamics, Institute of Geophysics, ETH Zurich, Sonneggstrasse 5, CH-8092 Zurich, Switzerland. (fabio.cramer@erdw.ethz.ch)